Simulation of the Braiding Process in LS-DYNA®

Seyedalireza Razavi[1] and Lorenzo Iannucci[1]
[1]*Imperial College London, Department of Aeronautics, London, UK*

Abstract

Textile braids and the over-braiding manufacturing technology have been attracting a lot of recent interest, particularly in the aerospace and automotive industries, in response to increasing demands for a low cost manufacturing process to produce high-performance composites. The application areas extend from the over-braided structural components of super-cars (e.g. Lamborghini Aventador) to 2D and 3D triaxial braided composite fuselages, wings, and circumferential frames of the transport aircraft. Thus with such potentials, it is essential to use virtual simulation tools to predict final mechanical properties of the textile preforms through resembling the actual braiding process condition before the part is physically fabricated.

In this study, an FE-based approach to simulate the braiding process has been developed using the explicit FE-code LS-DYNA. Two triaxial braid architectures were created by accounting for the fiber-to-fiber and fiber-to-mandrel static and dynamic friction coefficients. The aim was to compare the morphology and tensile strain behaviour of the created FE-models with the experimentally observed features of a fabricated braid prototype.

Preliminary results show that the braid angle, as a characteristic "fingerprint" of any braid architecture, is simulated with a close correlation to the fiber orientation angle of the braided prototype, which was produced during the actual braiding process and tensile tested experimentally. This implies that the FE-model developed in this work can be a potentially promising approach to create different triaxial braid preforms and to predict the final geometrical properties of complex composite tubular braids, depending on the shape of the mandrel used during the virtual over-braiding process.

1 Introduction

Textile composites are widely used in automotive and aeronautic industries due to their outstanding mechanical properties (e.g., high specific energy absorption (SEA)) and the ability to adapt to a wide range of tailor-design engineering applications [1]. One important example in this regard is composite shafts, which have emerged as a new application paradigm to replace aluminum/steel constituent for automotive drive shafts, helicopter propeller, and high-speed air spindles [2-4]. To date, braiding has been used as one of the most common and versatile textile fabricating technique for the manufacture of composite shafts. In particular, 3D-braiding is fast becoming an attractive method for the production of textile composites, since not only does it provide improved mechanical properties in the thickness direction of the braided structure, but it also allows the production of 'one-piece' solid braided profiles with varying cross sections to be possible during a single-run manufacturing process [5]. Nevertheless, there are a number of parameters involved in the braiding manufacturing process which can adversely affect final mechanical properties of the braided component. These include yarns alignment, braiding angle, number of yarns, friction, and take-up speed. Unfortunately, the prediction of the combined interaction of these parameters in each single braiding run is not straight forward and would require a large number of trial and error tests, especially in the cases when a large number of yarns are used [6].

Several studies have reported using both numerical and analytical models in the simulation of the braiding process to increase the reliability and cost-effectiveness of the manufacture of high-performance braided composites [7-10]. Although, the majority of the work has relied on either the prediction of yarn alignment in the final textile geometry – based on optical or microscopic observations of dry fabrics [11, 12], or the development of 2D and 3D models using computer-aided geometric design (CAGD) software [13, 14]. Adanur [15] developed an adaptive CAD model that was capable of generating different fabric geometries (e.g., braid or woven), based on translating the cross-sectional shape of the desire yarn along the yarn's axis. A CAD-based software, "TexGen (2012)" [16] was developed by the University of Nottingham, which generates 3D textile geometries for different preforms within a unit cell. The unit cell can then be used in the simulation of the fabrication process. Similarly, a 2D and 3D textile geometry modelling software, called Wisetex, was

developed by Lomov et al. [17] where, by the inputting analytical data regarding the physical properties of yarns within a textile structure, a multilevel geometry containing micro, macro, and meso –mechanical models of a complex shape could be created. Other studies involve the use of representative volume element (RVE) approach for determining mechanical properties and stress characterization of 3D-braided structures [18-23]. Dong and Huo [24] studied the effect of pore defects on two-scale finite element (FE) models of the fiber tows and the braided composites in ANSYS. Lei et al. [25] investigated the tensile properties of representative volume cell (RVC) of a three-dimensional four-directional braided composite using ABAQUS finite element code.

In many of these references a great deal of effort has been made to predict elastic properties and the failure mechanism of triaxial braided structures, without accounting for the geometrical inconsistencies (e.g., fibers crimp and misalignment in the CAD models). In addition, the majority of work based on the RVE approach has assumed rectangular RVE unit cells [14], which are not particularly suitable for modelling cylindrical-shape triaxial braids. Alternatively, few studies which have considered cylindrical RVE geometries [23] (in addition to several other analytical models reporting the braiding process [26-29]), have often neglected yarns physical interaction or yarns-to-mandrel slippage as a function of the frictional properties of the interfaces [30].

2 The braiding process

As a part of the experimental work, a triaxial 1x1 Diamond braid prototype was fabricated using a Maypole-type Herzog® [31] rotary braiding machine [Fig. 1]. This type of machine was equipped with two operating heads, each having eight horn gears, and eight carriers; with the possibility of inserting an axial core mandrel through the center of each head. Half of the yarn carriers move in a counter-rotating and pseudo-sinusoidal fashion and at the point where two opposite-moving carriers meet, each yarn passes over and below the other yarn – forming the circumferential braid geometry around the mandrel. The yarns were made of a high-density thermoplastic polymer, each comprised of forty-eight filaments. A closely-packed yarn had an overall diameter of 0.151±0.14 mm. During the actual braiding process a solid metal core with a diameter of 0.4 mm was inserted in the axial direction of the tubular braid. The aim here was to fabricate this reference braid prototype and compare its morphological characteristics with those of the FE-models, which were created during the virtual braiding process simulations. In addition, important braiding parameters such as the take-up speed and the effect of the number of active bobbins on the braid angle[1], α, could be empirically measured and compared with the simulations.

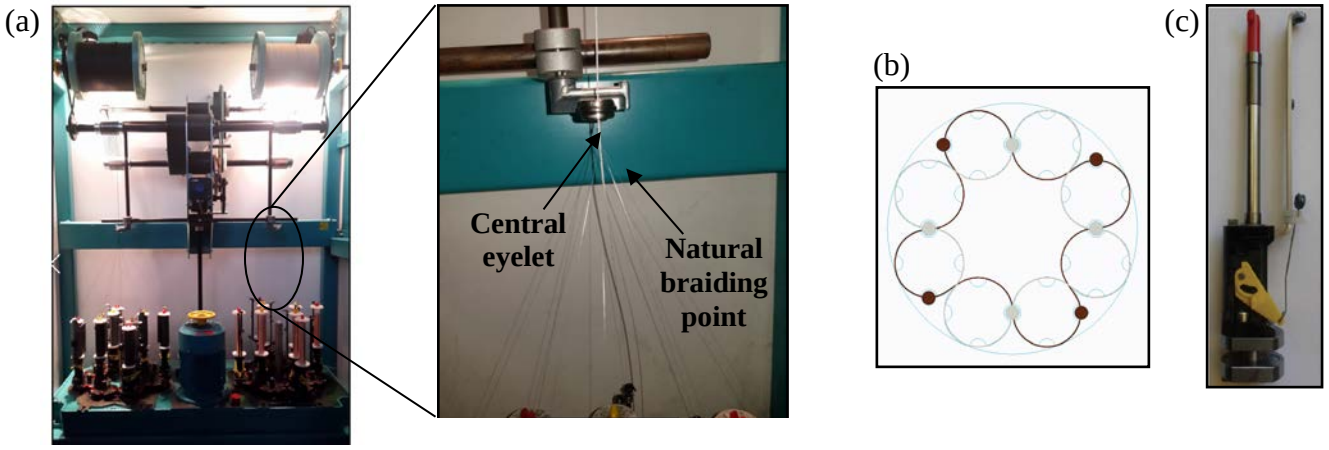

Figure 1. A maypole-type braiding machine in (a). A schematic top view of the horn gears and the carriers' path in (b); the yarn-carrier which enhouses a downward tension spring in (c).

[1] The braid angle is defined as the angle formed "between the braid axis and the yarn axis" [32].

3 The FE simulation of the braiding process

The FE model of the braiding process was simulated in LS-DYNA [Fig. 2]. Using the analytical functions derived in [32], it was possible to calculate the exact coordination points of each carriers' path during the braiding process at every 0.01s interval. These coordination points were used as an input file in LS-PrePost®, under the card: ***Define** > **Curve**. Similar to the work performed in [33], the constituent fibers were modelled with 2D-Beam elements. The virtual diameter of each beam part was defined equivalent to the diameter of each individual fiber within the actual yarn. For the sake of simplicity, some of the parametric "Keywords" input files are summarized in [Table 1] below.

Keywords	Input	Type (**units)
***BOUNDARY**	SPC_SET	
	PRISCRIBED_MOTION_SET	
***CONTACT**	*CONTACT_AUTOMATIC_GENERAL	Yarn-to-Yarn
	*CONTACT_AUTOMATIC_BEAMS_TO_SURFACE Option Card: A_SOFT=1	Yarn-to-Mandrel
	*CONTACT_AUTOMATIC_BEAMS_TO_SURFACE	Yarn-to-Eyelet
***CONTROL**	ENERGY	HGEN: 1
	HOURGLASS	IHQ: 1
	TERMINATION	2300ms
	TIMESTEP	TSSFAC: 0.2
***DATABASE**	BINARY_D3PLOT	DT: 2.5
***ELEMENT**	SHELL	Eyelets
	SOLID	Mandrel
	BEAM	Fibers
***MAT**	PIECEWISE_LEANER_PLASTICITY	Fibers
	ELASTIC	Eyelets
	RIGID	Mandrel
	SPRING_ELASTIC	Discrete elements
***SECTION**	SHELL	Eyelets
	SOLID	Mandrel
	BEAM	Fibers

********Units are in: kg, mm, and ms.*

According to the manufacturer [31, 34], the coefficient of static and dynamic frictions (**FS** and **FD**) for the "yarn-to-eyelet" and "yarn-to-mandrel" were set to 0.1 and 0.05, respectively. The braid take-up speed was defined as an upward displacement motion in ***Prescribed_Motion_Set** boundary condition. The carriers' spring tension were modelled as ***Element_Discrete**, by defining a constant downward mass of 0.1 kg via ***Element_Mass** card option.

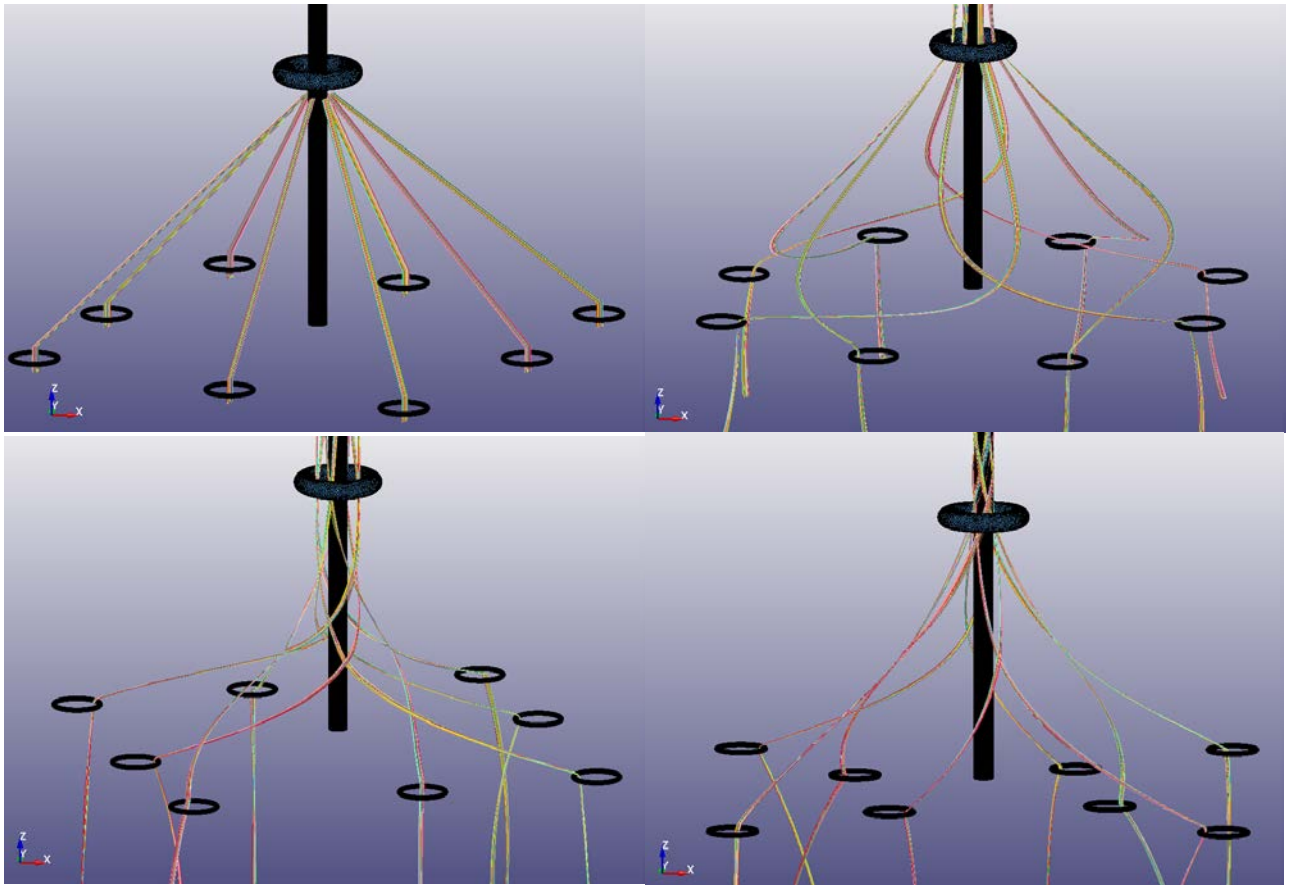

Figure 2. The braiding process simulation in LS-DYNA.

3.1 The braid geometry

In order to demonstrate the adaptability of the proposed FE model to different core geometries, two scenarios were examined. The first model was created analogous to the previously-fabricated braid prototype by using a cylindrical core. The second model involved the yarns over-braiding an arbitrary mandrel shape, a rectangular core. The material properties and braiding parameters were the same in both models (as in Table 1). The FE-simulation results are visualized in [Fig. 3].

3.2 The braid angle

To assess whether and how realistic is the produced FE-simulated braid architecture, both the FE-model and the fabricated braid prototype were subjected to a displacement loading condition. The former braid was tensile tested in LS-DYNA, by having one ends of the fibres fixed via ***SPC_SET** boundary condition, while having the other ends subjected to a constant-velocity displacement boundary condition, via ***Prescribed_Motion_Set** option. The latter braid was tensile tested experimentally using a 50kN Instron tensile test machine with an axial deformation of 10 mm at an extension rate of 1 $mm.min^{-1}$. Sample preparation procedure followed the outline in [35] – in accordance ASTM D3822-07 Standard Test Method for Tensile Properties of Single Textile Fibers [36]. The results regarding the tensile strain behaviour of the braids are shown in [Fig. 4].

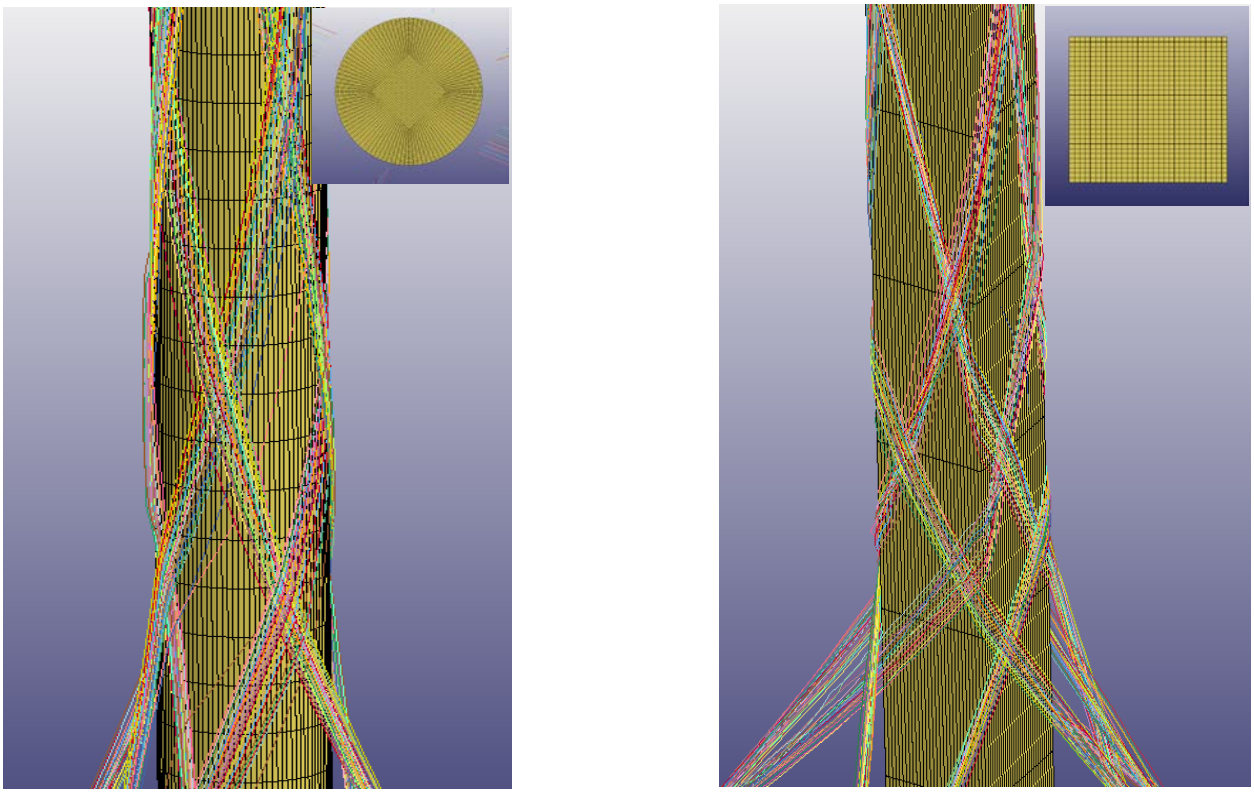

Figure 3. Schematics of the over-braiding process, over (a): a cylindrical core and (b): a rectangular core mandrel.

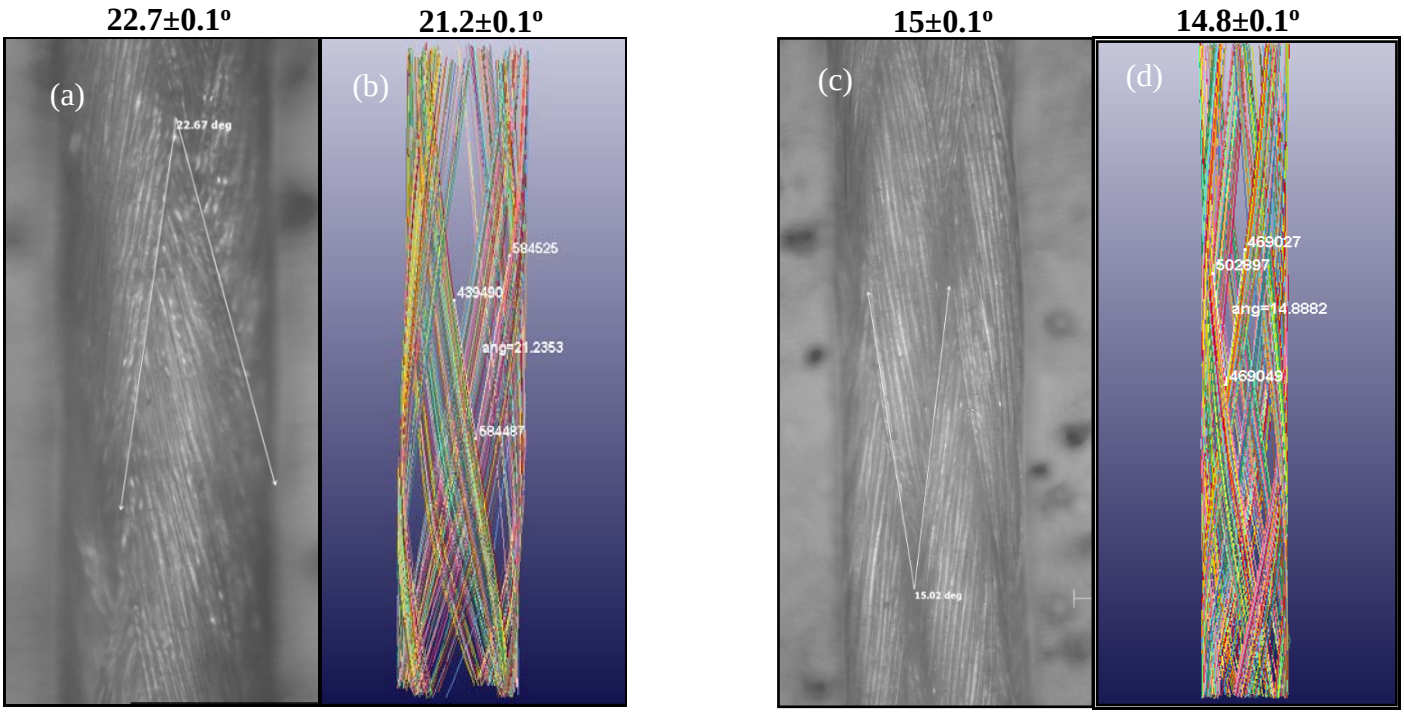

Figure 4. The braid angle and tensile behaviour of the yarns. (a) and (b): the actual and FE-simulated braids before the tensile loading; (c) and (d): the actual and FE-simulated braids after the tensile loading.

Interestingly, as it can be seen from [Fig. 4], at interlacement points each fiber has remained parallel with respect to its neighbouring fibers – similar to the braid pattern observed within the fabricated prototype [Fig. 5]. This can confirm the accuracy of the contact definitions used for the fiber-to-fiber and fiber-to-mandrel contacts. Nevertheless, a major shortcoming of the current FE-model can be said to be the presence of some periodic gaps in the braid pattern. Although, this issue can be explained by three important elements that have not been modelled in the FE-simulations. First, having an unequal number of constituent fibers within each FE-modelled yarn as compared to the actual number of fibers existing within the physical yarns. Second, modelling each fiber as beam elements instead of using Shell or Solid elements – in order to reduce the computational time – which in turn would not allow the fibers to exhibit their natural tendency to "flatten" under the pressure; and third, an unrealistic dispersion of the constituent fibers across the cross-sectional area of the yarns in the FE-model [Fig. 6].

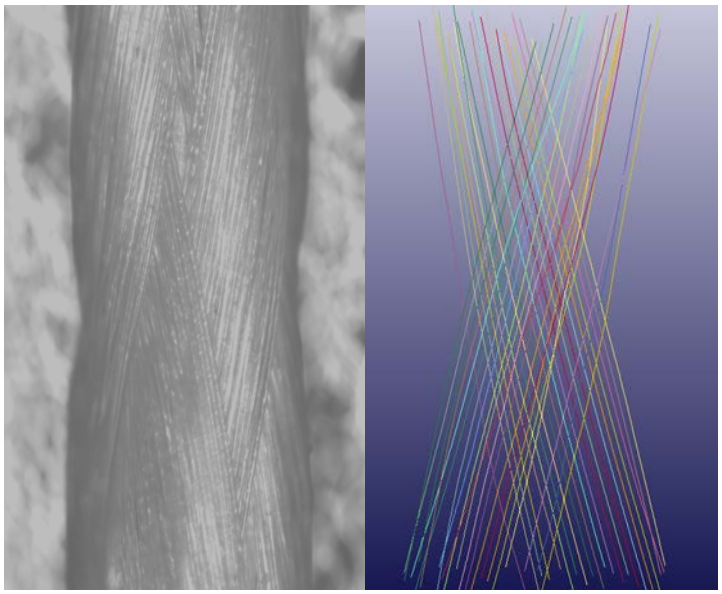

Figure 5. Braids interlacement pattern in (a): actual braid, (b): FE-model.

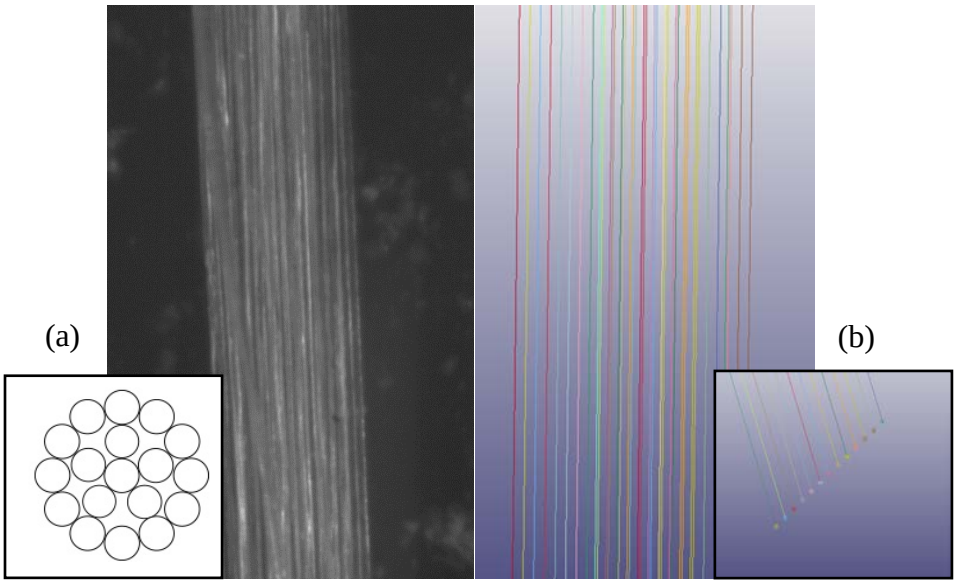

Figure 6. Schematic views of the yarns and their cross sectional areas. (a): the actual yarn; (b): the FE-modelled yarn with a simplified linearly aligned cross section.

4 Summary

The aim of the present study was to develop a FE-based adaptable approach to model the braiding process of different tubular preforms in LS-DYNA. Using this approach, two triaxial braid architectures were simulated successfully, by over-braiding eight multifilament yarns around a rectangular and a circular mandrel. The mandrels, which are metal cores in the experiment, were represented in the FE-models as a ***Solid** > **Rigid_Body**.

The yarns were modelled by as many beam elements as computationally efficient, in order to enable them to realistically bend around the curve surfaces and stay fully in contact with the mandrel whilst sliding upwards due to the take-up speed. The FE-model inputs regarding the braiding process parameters and the yarn properties were obtained experimentally from the actual braiding manufacturing process and via microscopic image analysis of the yarn's morphology.

Fiber orientation angle of the naturally-produced braid as well as the tensile tested (deformed) braid in the FE-models agreed well with the experiments. Although, it was also observed that by increasing the number of fibers from twenty one to about thirty four, the estimated computational time required to solve the fiber-to-fiber contact algorithms increased by a factor of two, to about 6 hours. Therefore, at this stage, the braiding process was simulated with limiting the maximum number of fibers in each yarn to only twenty-one filaments.

However, as a part future work, we are working on the optimization of the braiding process parameters (such as the take-up speed and the carriers rotary speed) and simplifications of some parts of the current FE-models (e.g. the eyelets material, sections, and properties), in order to allow the possibility to simulate complex triaxial performs with a large number of fibers while still maintaining a reasonable computational time.

References

1. Lin, S. and S. Poster. *Development of a Braided-Composite Drive Shaft with Captured End Fittings*. in *60th Annual Forum of the American Helicopter Society International*. 2004.
2. Bang, K.G., *Design of carbon fiber composite shafts for high speed air spindles.* Composite Structures, 2002. **55**(2): p. 247-259.
3. Kim, H.S., J.W. Kim, and J.K. Kim, *Design and manufacture of an automotive hybrid aluminum/composite drive shaft.* Composite structures, 2004. **63**(1): p. 87-99.
4. Reddy, P.S.K. and C. Nagaraju, *Weight optimization and Finite Element Analysis of Composite automotive drive shaft for Maximum Stiffness.* Materials Today: Proceedings, 2017. **4**(2): p. 2390-2396.
5. Tolosana, N., et al. *Development of a simulation tool for 3D braiding architectures*. in *AIP Conference Proceedings*. 2007. AIP.
6. Boisse, P., *3 - Finite element analysis of composite forming A2 - Long, A.C*, in *Composites Forming Technologies*. 2007, Woodhead Publishing. p. 46-79.
7. Lomov, S.V., et al., *Textile composites: modelling strategies.* Composites Part A: applied science and manufacturing, 2001. **32**(10): p. 1379-1394.
8. Monnot, P., J. Lévesque, and L. Laberge Lebel, *Automated braiding of a complex aircraft fuselage frame using a non-circular braiding model.* Composites Part A: Applied Science and Manufacturing, 2017. **102**: p. 48-63.
9. Zhou, H., et al., *Finite element analyses on transverse impact behaviors of 3-D circular braided composite tubes with different braiding angles.* Composites Part A: Applied Science and Manufacturing, 2015. **79**: p. 52-62.
10. Shanahan, C., S.A.M. Tofail, and P. Tiernan, *Viscoelastic braided stent: Finite element modelling and validation of crimping behaviour.* Materials & Design, 2017. **121**: p. 143-153.
11. Rawal, A., A. Sibal, and H. Saraswat, *Tensile behaviour of regular triaxial braided structures.* Mechanics of Materials, 2015. **91**: p. 277-289.
12. Rawal, A., et al., *Geometrically controlled tensile response of braided sutures.* Materials Science and Engineering: C, 2015. **48**: p. 453-456.
13. Shen, Y., et al., *Finite element analysis of monofilament woven fabrics under uniaxial tension.* The Journal of The Textile Institute, 2015. **106**(1): p. 90-100.
14. Ma, W., Z. Ma, and J. Zhu, *Processing technique and geometric model of an imperfect orthogonal 3D braided material.* Journal of Industrial Textiles, 2016: p. 1528083716644291.

15. Adanur, S. and T. Liao, *3D modeling of textile composite preforms.* Composites Part B: Engineering, 1998. **29**(6): p. 787-793.
16. Sherburn, M., *Geometric and mechanical modelling of textiles*. 2007, University of Nottingham.
17. Verpoest, I. and S.V. Lomov, *Virtual textile composites software WiseTex: Integration with micro-mechanical, permeability and structural analysis.* Composites Science and Technology, 2005. **65**(15): p. 2563-2574.
18. Dong, J. and N. Huo, *Progressive tensile damage simulation and strength analysis of three-dimensional braided composites based on three unit-cells models.* Journal of Composite Materials, 2017: p. 0021998317737828.
19. Nagai, K., et al., *The stress analysis method for three-dimensional composite materials.* Applied Composite Materials, 1994. **1**(3): p. 197-216.
20. Ansar, M., W. Xinwei, and Z. Chouwei, *Modeling strategies of 3D woven composites: a review.* Composite structures, 2011. **93**(8): p. 1947-1963.
21. Kuo, W.-S. and B.-J. Pon, *Elastic moduli and damage evolution of three-axis woven fabric composites.* Journal of materials science, 1997. **32**(20): p. 5445-5455.
22. Hao, W., et al., *Computational analysis of fatigue behavior of 3D 4-directional braided composites based on unit cell approach.* Advances in Engineering Software, 2015. **82**: p. 38-52.
23. Hao, W., et al., *A unit-cell model for predicting the elastic constants of 3d four directional cylindrical braided composite shafts.* Applied Composite Materials, 2017: p. 1-15.
24. Dong, J. and N. Huo, *A two-scale method for predicting the mechanical properties of 3D braided composites with internal defects.* Composite Structures, 2016. **152**: p. 1-10.
25. Lei, B., et al., *Bearing abilities and progressive damage analysis of three dimensional four-directional braided composites with cut-edge.* Applied Composite Materials, 2016. **23**(4): p. 839-856.
26. Guyader, G., A. Gabor, and P. Hamelin, *Analysis of 2D and 3D circular braiding processes: Modeling the interaction between the process parameters and the pre-form architecture.* Mechanism and Machine Theory, 2013. **69**: p. 90-104.
27. van Ravenhorst, J.H. and R. Akkerman, *Circular braiding take-up speed generation using inverse kinematics.* Composites Part A: Applied Science and Manufacturing, 2014. **64**: p. 147-158.
28. Pickett, A.K., J. Sirtautas, and A. Erber, *Braiding simulation and prediction of mechanical properties.* Applied Composite Materials, 2009. **16**(6): p. 345.
29. Pickett, A., et al., *Comparison of analytical and finite element simulation of 2D braiding.* Plastics, Rubber and Composites, 2009. **38**(9-10): p. 387-395.
30. Hans, T., et al., *Finite element simulation of the braiding process for arbitrary mandrel shapes.* Composites Part A: Applied Science and Manufacturing, 2015. **77**: p. 124-132.
31. HERZOG^{R}, *August Herzog Maschinenfabrik GmbH & Co. KG*, H. Flechtmaschinen, Editor. 2012, Herzog Flechtmaschinen: Germany.
32. Del Rosso, S., *Micro-scale Hybrid Fibres for Low Cost Polymer Armours*, in *Aeronautics*. 2014, Imperial College London: London. p. 239.
33. Vinot, M., M. Holzapfel, and C. Liebold, *Investigating the influence of local fiber architecture in textile composites by the help of a mapping tool.* 2017.
34. Solef, S., *PVDF Design & Processing Guide*. 2017.
35. Bhagwat, V.K.K., *Testing of High Performance Polymers*. 2016, Imperial College London: London. p. 107.
36. *Standard Test Method for Tensile Properties of Single Textile Fibers.*